Journal of Clinical Immunology, Vol. 24, No. 4, July 2004 (© 2004)

Griscelli Syndrome: Characterization of a New Mutation and Rescue of T-Cytotoxic Activity by Retroviral Transfer of *RAB27A* Gene

JOÃO C. S. BIZARIO,[1,2] JÉRÔME FELDMANN,[3] FABÍOLA A. CASTRO,[4,5] GAËL MÉNASCHÉ,[3] CRISTINA M. A. JACOB,[6] L. CRISTOFANI,[6] ERASMO B. CASELLA,[6] JÚLIO C. VOLTARELLI,[5] GENEVIÈVE DE SAINT-BASILE,[3] and ENILZA M. ESPREAFICO[1,7]

Accepted: March 2, 2004

Griscelli syndrome (GS) is caused by mutations in the *MYO5A* (GS1), *RAB27A* (GS2), or *MLPH* (GS3) genes, all of which lead to a similar pigmentary dilution. In addition, GS1 patients show primary neurological impairment, whereas GS2 patients present immunodeficiency and periods of lymphocyte proliferation and activation, leading to their infiltration in many organs, such as the nervous system, causing secondary neurological damage. We report the diagnosis of GS2 in a 4-year-old child with haemophagocytic syndrome, immunodeficiency, and secondary neurological disorders. Typical melanosome accumulation was found in skin melanocytes and pigment clumps were observed in hair shafts. Two heterozygous mutant alleles of the *RAB27A* gene were found, a C-T transition (C352T) that leads to Q118stop and a G-C transversion on the exon 5 splicing donor site (G467+1C). Functional assays showed increased cellular activation and decreased cytotoxic activity of NK and CD8+ T cells, associated with defective lytic granules release. Myosin-Va expression and localization in the patient lymphocytes were also analyzed. Most importantly, we show that cytotoxic activity of the patient's CD8+ T lymphocytes can be rescued *in vitro* by RAB27A gene transfer mediated by a recombinant retroviral vector, a first step towards a potential treatment of the acute phase of GS2 by RAB27A transduced lymphocytes.

KEY WORDS: Immunodeficiency diseases; Griscelli syndrome; cell trafficking; CTL; gene therapy.

INTRODUCTION

Griscelli syndrome (GS, MIM 214450) is a rare, fatal, autosomal recessive disorder, first described as a partial albinism associated with immunodeficiency (1, 2). Symptoms and evolution of this disease are quite variable and involve the pigmentary, immunological, and neurological systems. Pigmentary defects are always present in GS patients, characterized by hypopigmentation due to the accumulation of melanosomes in the perinuclear region of the melanocytes, thus impairing the transfer of these granules to the keratinocytes, resulting in a silvery-gray color of the hair and pigmentary dilution of the skin (3). Immunological features include susceptibility to repeated infections and deficiency of T cell cytotoxic activity, which leads to the occurrence of haemophagocytic syndrome (HS), a condition also referred to as the "accelerated phase." HS is often fatal and characterized by periods of fever, pancytopenia, lymphocyte and macrophage activation, and lymphocyte hyperproliferation, leading to infiltration of spleen, liver, lymph nodes, and brain (4–6). HS usually leads to a secondary neurological involvement, characterized by episodes of convulsion, hemiparesis, neuropsychomotor involution and may include other symptoms, such as loss of cognitive memory and fatal neural degenerations (7). Pastural *et al.* (8) reported the first gene involved in this disease, *MYO5A*, mapped on chromosome 15q21. This is the equivalent of the *dilute*

[1]Departamentos de Biologia Celular, Molecular e Bioagentes Patogênicos, São Paulo, Brazil.
[2]Departamentos de Curso de Medicina da Universidade de Ribeirão Preto (UNAERP), São Paulo, Brazil.
[3]Departamentos de Unité de Recherches sur le Dévelopement Normal et Pathologique du Système Immunitaire, INSERM U-429, Paris, France.
[4]Departamento de Análises Clínicas, Toxicológicas e Bromatológicas da Faculdade de Ciências Farmacêuticas de Ribeirão Preto-USP, São Paulo, Brazil.
[5]Departamentos de Clínica Médica da Faculdade de Medicina de Ribeirão Preto-Universidade de São Paulo (USP), Brazil.
[6]Departamento de Pediatria da Faculdade de Medicina-USP, São Paulo, Brazil.
[7]To whom correspondence should be addressed at Av. Bandeirantes, 3900, 14049-900 Ribeirão Preto–SP–Brazil; e-mail: emesprea@fmrp.usp.br.

0271-9142/04/0700-0397/0

locus in mice (9) and encodes myosin-Va, a molecular motor of the unconventional myosin superfamily, involved in the short-range transport or positioning of vesicles, organelles, mRNA and other cellular factors in many cell types (10–12). Pastural *et al.* (13) and Ménasché *et al.* (4) described a second gene, *RAB27A*, located next to the *MYO5A* locus, whose mutation accounts for most cases of GS reported. This is the equivalent of *ashen* locus in mice (14) and encodes Rab27a, a small GTPase of the Ras superfamily, involved in targeting-docking-fusion of vesicles and organelles in eukaryotic cells (15, 16). These works led to the subdivision of this syndrome in two groups, GS1, caused by mutation in the *MYO5A* gene, and GS2, in the *RAB27A* gene. Both of them show the pigmentary features, whereas blood dysfunctions are only observed in GS2 patients, and primary severe neurological involvement in GS1. However, GS2 patients usually develop neurological complications secondarily to the HS (6, 7). Bone marrow transplantation (17, 18) and chemotherapy (19, 20) have been applied in GS2 patients with some success. The lack of immunological involvement in patients with *MYO5A* mutations has also led to the suggestion that *MYO5A* mutations would be better classified within another abnormality condition called Elejalde syndrome (ES [MIM 256710]), a neuroectodermal melanolysosomal disease characterized by pigmentary defects similar to GS and severe primary neurological dysfunctions, with seizures, hypotonia, and mental retardation (21).

It is interesting to point out that a great deal of information has been made available from recent studies on the molecular basis of the three phenotypically similar coat color mutations in mice, *dilute*, *ashen*, and *leaden*, as well as human GS. Leaden encodes a rabphilin-like protein that was designated melanophilin and functions as a Rab27a effector in melanocytes (22). Very recently a third form of Griscelli syndrome (GS3) was shown to result from melanophilin defect (23). In this case, the GS phenotype is restricted to the characteristic hypopigmentation of this disease. Rab27a is targeted to the melanosome membrane after prenylation and binds to melanophilin in a GTP-dependent manner. Melanophilin then recrutes the molecular motor myosin-Va, which allows movement or tethering of the melanosomes on the actin cytoskeleton (3, 24–28). These findings explain the common pigmentary features observed in GS1, GS2, and GS3 patients, and the distinct features are in part due to tissue specific expression of these genes. While all three proteins are expressed in melanocytes, only myosin-Va is highly expressed in neurons. In lymphocytes, Rab27a is highly expressed, whereas melanophilin and myosin-Va has not been detected in cytotoxic T lymphocytes (29), despite that myosin-Va has been detected in leukocytes (30–32), in all mononuclear cell subtypes (33). Although not yet clarified, an alternative Rab27a effector, potentially capable of recruiting a class V myosin member and/or another member of the myosin superfamily, is likely to function in lymphocytes (34), explaining the lack of immunological dysfunctions in GS1 and GS3 patients or in *dilute* and *leaden* mice (4, 23, 29, 35). The immune defects of GS2 patient have been attributed to the lack of cytotoxic activity of CD8+ T lymphocytes due to a deficient lytic granules release in these cells (4, 35, 36). In fact, genetically determined cytotoxic defect resulting from *perforin* mutation in patients with familial hemophagocytic syndrome (FHL) leads to identical immune phenotype as the one observed in GS2 patients (37). In the present work, we report two mutant alleles of the *RAB27A* gene found in a Brazilian child and describe the clinical and cellular features of the disease in this patient. We also show analyses of myosin-Va expression and localization in the patient's lymphocytes. In addition, we demonstrate *in vitro* rescue of CD8+ T lymphocyte cytotoxic activity using a retroviral vector mediated *RAB27A* gene transfer.

PATIENT AND CONTROLS

Case Report

A male Brazilian patient was the first child of nonconsanguineous parents. At birth he presented silvery-gray hair (Fig. 1A) and postnatal jaundice treated with phototherapy. At 5 months he was referred to the Children's Institute of the Faculty of Medicine of the University of São Paulo (ICrHCFMUSP), presenting fever, hepatosplenomegaly, and pancytopenia. Agnogenic myeloid metaplasia was diagnosed and treated with corticosteroids. He remained with recurrent fever episodes including three pneumonias and cytopenias, such as neutropenia and thrombocytopenia and bone marrow smears haemophagocytosis. During the first 4 years he showed normal psychomotor development, but at 4-years-old he presented repeated convulsive episodes, hemigeneralized, remaining in the intensive care unit during 45 days. A CT scan revealed right parieto-occipital edema, diffuse infiltration in the left putamen and bilateral cortex. Then, neuropsychomotor status deteriorated, with appearance of bilateral hemiparesis predominating on the left side. In addition, his motor coordination, equilibrium and speech were impaired, associated with multiple convulsive episodes. The hypothesis of Chèdiak-Higashi syndrome (CHS) diagnosis was ruled out because of the absence of giant intracellular granules in peripheral blood granulocytes. Then, the

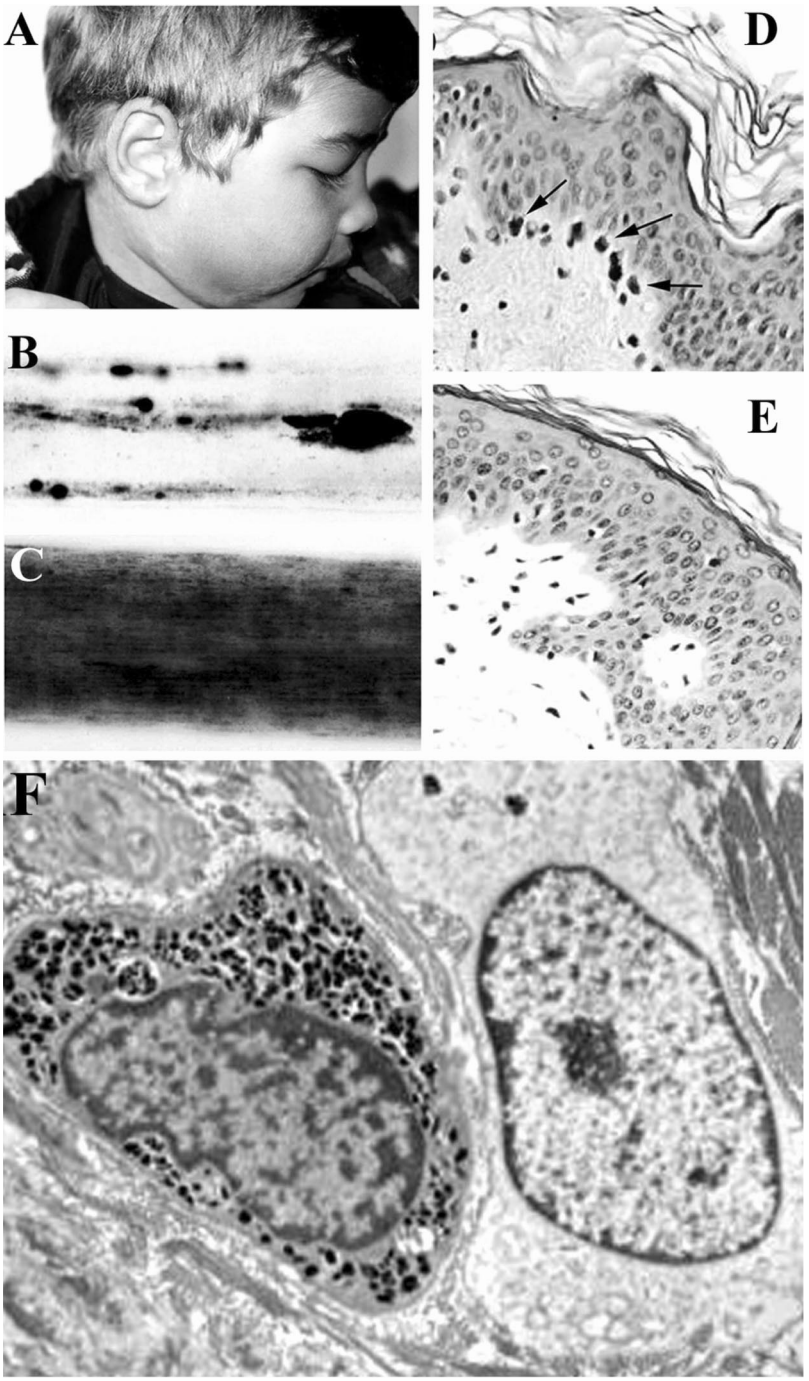

Fig. 1. Altered pigment distribution in the hair and skin from the patient with *RAB27A* mutation. (A) Patient PO. Note the silvery-gray color of the hair, eyelashes, and eyebrows. (B and C) Optical microscopy images of hair samples from the patient (B) and a healthy individual (C). Note the aggregates of pigment and empty areas within the hair shaft. (D and E) HE stained skin sections from the patient (D) and a healthy individual (E). Note the accumulation of brown pigment in cells present in the basal layer of the epidermis (D, arrows). (F) Electron-microscopy image depicting a melanocyte with a large accumulation of mature melanosomes in the perinuclear region. [Note: The on-line version of this figure appears in color.]

accelerated phase of Griscelli disease was suggested as a possible diagnosis. Morphofunctional and molecular diagnoses of GS were done and are presented here. No familial HLA compatible donor was identified and bone marrow transplantation was excluded as a treatment option. Immunosuppressor agents, including corticosteroid associated to cyclosporine, and antithymocyte immunoglobulin sustained a clinical remission until 7-years-old when a second accelerated phase developed and the patient was put in an induced coma for 20 days. Convulsive episodes and recurrent infections were observed during the evolution of the disease. The same treatment was applied, but the patient continued with deterioration of his neurological conditions. At the beginning of a new accelerated phase, standard chemotherapy protocol was applied. The patient did not respond to this treatment and died from multiple organ failure at 9-years-old. Note: Blood samples and skin fragment from the patient were collected only after obtaining of an informed consent to the investigations from his parents.

Controls

A group of patients was selected, during routine sample collection at the ICrHCFMUSP. Children from 4- to 8-years-old with no immunodeficiency, or any other diseases which could interfere with the tests, were submitted to blood collection after the signature of an informed consent by their parents. We also used samples obtained from 19 consenting adult donors from the Regional Blood Center Foundation of Ribeirão Preto – SP – Brazil.

MATERIAL AND METHODS

Optical Microscopy

Skin fragments were fixed with 4% glutaraldehyde in 0.1 M cacodylate buffer, pH 7.4, for 24 h, at 4°C. After washing 3 times with the same buffer, the fragments were processed by routine histological procedures and stained with hematoxylin-eosin. Hair samples were observed without any previous treatment. Photomicrographs were obtained using an AXYOPHOT-ZEISS (Jena, Germany) microscope.

Electron Microscopy

Skin fragments were fixed as described above and post-fixed in 1% osmium tetroxide in cacodylate buffer, for 1 h, at 4°C, and transferred to 1% uranyl acetate in 0.1 M sodium acetate, pH 5.0, on ice, overnight. Fragments were then gradually dehydrated in ethanol and embedded in araldite. Ultrathin sections were taken and placed on pioloform-coated copper grids, contrasted with 2% uranyl acetate for 20 min, 0.3% lead acetate for 3 min, and observed under a Philips electron microscope, model EM-208.

Cell Isolation

Peripheral blood mononuclear cells (PBMC) were isolated from whole heparinized blood by Ficoll-Hypaque density-gradient technique (Hystopaque-1077; Sigma, St. Louis, USA).

Mutation Detection

DNA and RNA were isolated from PBMC following standard procedures. Myosin-Va cDNAs were obtained by reverse transcription using Superscript-II enzyme (GIBCO-BRL, Carlsbad, USA) and PCR using the enzyme ELONGASE (GIBCO-BRL, Carlsbad, USA) or Taq DNA polymerase (PHARMACIA, Uppsala, Sweden, USA), using the following pair of primers: 5′-GCC CTG CCC TGC CCT GCT C-3′ and 5′-AGA CTC GTT GCT GCT GTG G-3′, to amplify from nucleotide 131 to 3616, a cDNA fragment which encodes the head, neck, and proximal tail domain of myosin-Va; and 5′-CCA CTG GGC GGG TCC TT-3′ and 5′-TGG TGC CTT CCT AAC AAC AGC-3′, to amplify from nucleotide 3192 to 6212, which encodes from the proximal tail to the STOP codon. For amplification of the Rab27a gene, we used primers designed from intronic sequences flanking exons 2 to 6 of RAB27A, which encodes the whole open reading frame, to amplify genomic DNA from the patient, his brother and parents. Standard Taq DNA polymerase and the following pair of primers were used, respectively: 5′-TCA TAC AAC CCT AGA CAT ACA-3′ and 5′-TGT TGA CTT AAC GAT TAC ATT TTT-3′; 5′-TTG TTT TCT CTT TCA CTT G-3′ and 5′-TTT TCC CTT TCC TTC AG-3′; 5′-GCT GAA GGC ATT GCT TGT-3′ and AGA TCT CCT CCA AAA CGA TT-3′; 5′-TTT TGC ATG TAT TGT TCA CTG A-3′ and 5′-TG GCT GAG GTT TTG CTT TA-3′; 5′-TGT CTT CCA GAA TCC CCT ACT-3′ and 5′-ATG CCC ATT AAT CTC TCA CTG T-3′.

Sequencing

Direct sequencing of the PCR products was performed using the Big DyeDeoxy terminator kit RR Mix protocol and an ABI 377 sequencer (Applied Biosystems, Foster City, USA). Sequences were aligned with the RAB27A (genomic contig: NT_010194; mRNA sequence: NM_183236) or MYO5A (NM_000259) sequences obtained from GENBANK.

Genotype Analysis Using Polymorphic Markers

Primers against CHLC.GCT1E8, D15S1049, and D15S121 polymorphic regions, located within the *RAB27A* locus, on chromosome 15q21, were used, as described by Ménasché *et al*. (3). Radioactive PCR was performed to amplify the polymorphic regions. Labeled PCR products were subjected to electrophoresis in polyacrylamide gel, in order to separate the fragments obtained. An X-ray film (Kodak, Rochester, USA) was exposed to the gel and the developed bands were analyzed and enumerated on the basis of the relative migration, from the top to the bottom of the gel.

Proliferation Assays Upon Mitogen Stimulation and Mixed Lymphocyte Culture

For the mitogen stimulus, 100 μL of 2×10^6 cells/mL suspension were incubated in the presence of 2.5 μg/mL Phytohemagglutinin (PHA) or 3 μg/mL Concanavalin A (Con-A) (both lectins were from Sigma, St. Louis, USA), for 72 h. Then, all cultures were pulsed with 1 μCi/well ^{3}H-Thymidine (Amersham, Buckinghamshire, UK) and incubated for an additional 24 h period, in the same conditions as specified above. Cells were then harvested and β-emission, in counts per minute (cpm), was measured in a β-counter (Beckman LS8100, Fullerton, USA). All assays were performed on triplicate. Stimulation Index was determined by the ratio of cpm in the mitogen-stimulated samples to cpm in nonstimulated samples. Two-way mixed lymphocyte culture was performed according to standard protocols (38), using cells from the patient and unrelated control individuals. Freshly isolated peripheral blood mononuclear cells were ressuspended in RPMI-1640, supplemented with 20% human AB serum in a density of 1×10^6 cell/mL. For the mixed culture, samples of a 100 μL of cell suspensions (1×10^5 cells) from each individual, the patient and an unrelated individual or from two unrelated controls, were plated in a 96-wells round bottom microtiter plate and incubated in a humidified atmosphere with 5% CO_2, at 37°C, during 5 days. To determine the background level of ^{3}H-Thymidine incorporation, the same number of cells (2×10^5) was plated separately for each individual, and to determine the maximal proliferation levels, a pool of 2×10^5 cells from 5 unrelated individuals were plated. Within the fifth day of incubation, cultures were pulsed with 0.5 μCi ^{3}H-Thymidine and incubated for an additional 18 h period, following which cells were harvested on filter paper and β-emission (cpm) was measured. The relative response was determined according to the formula: (test cpm – autologous cpm)/(pool cpm – autologous cpm) $\times$ 100. Where "autologous cpm" corresponds to spontaneous proliferation and "pool cpm" is the maximal proliferation from the pool of five unrelated cells.

Immunolabeling and Flow Cytometry

For HLA-DR staining, cells from the patient and six healthy chidren were simultaneously labeled with a Fluorescein Isothiocyanate (FITC)-conjugated monomorphic antibody to HLA-DR (clone L243) and a PE-conjugated antibody to CD3 (SK7), CD14 (MϕP9), and CD19 (SJ25C1) markers, respectively, each one at 10 μg/mL. Three independent assays were done for the patient and controls.

For myosin-Va staining, mononuclear cells from the patient and from 19 health adult blood donors were used. The detailed procedure employed here and the results of myosin-Va fluorescence intensity for the 19 healthy donors have been previously reported (29). Briefly, freshly isolated cells (100 μL, 5×10^6 cells/mL) were labeled with Phycoerytrin-conjugated monoclonal antibodies against the following human CD markers: CD3 (clone SK7), CD4 (SK3), CD8 (SK1), CD16 (Leu 11C), CD19 (SJ25C1), CD56 (NCAM16.2), and CD14 (MϕP9). Cells were then washed in Phosphate buffer saline (PBS), pH 7.2, fixed and permeabilized in the same buffer containing 2% paraformaldehyde and 0.01% Saponin, during 10 min, at 37°C. After washing (3×), cells were blocked for 1 h in PBS containing 2% BSA and 5% goat serum, followed by incubation with a polyclonal antibody against the tail domain of myosin-Va (39), at 10 μg/mL, for 1 h, at room temperature (RT), washing and incubation with a FITC-conjugated goat anti-rabbit IgG (Molecular Probes, Eugene, USA), also at 10 μg/mL, for 1 h, at RT. Antibodies to CD markers and HLA-DR were obtained from Becton-Dickinson, San Jose, USA. A single experiment was performed for the patient and controls.

As a control for nonspecific staining and to set the background levels, cells were labeled, under the same conditions specified above, with PE and FITC-conjugated γ2a/γ1 antibodies (clones X39/X40). Flow cytometry analyses were carried out on a FACSORT equipment (Becton-Dickinson, San Jose, USA), using a linear amplifier with resolution of 1024 units and the CELLQUEST analysis software. Fluorescence intensity was measured in arbitrary units (number of channel shifting) in histogram plot on a 0–1023 linear scale, for 10,000 cells counted in the lymphocyte gate and 15,000 in the monocyte gate, per blood sample analyzed. The median of fluorescence intensity was calculated from 10,000 or 15,000 cells, subtracted from the background fluorescence, for each cell subpopulation from the patient and from each one of the control blood samples analyzed.

Immunolabeling and Confocal Microscopy

Cells were plated on Cell-Tak (Becton Dickinson, Franklin Lakes, USA)-treated glass coverslips inside 35 mm diameter Petri dishes. Cells were colabeled with monoclonal antibody to β-tubulin (Transduction Laboratories, Lexington, KY) and a polyclonal to myosin-Va tail (39), essentially as described above. Coverslips were mounted in 1 mg/mL *p*-phenylenediamine in 90% glycerol and PBS. Image aquisition and processing were done using a Leica TCS-NT Confocal System (Leica Microsystems GmbH, Mannheim, Germany). Two independent assays were performed for the patient cells and a control sample in parallel.

NK Activity

NK activity against K562 target cells was assessed by a flow cytometry assay (40), using the DIO (Molecular Probes, Eugene, USA) membrane dye to stain live K562 cells and propidium iodide (PI, Sigma, St. Louis, USA) nuclear dye to stain dead cells. Unstained effector cells (monocyte-depleted PBMC) and DIO-stained target cells (K562) were added to each of six polystyrene 12×75 mm assay tubes at effector:target ratios of 40:1, 20:1, 10:1, and 5:1. As control, two of the tubes contained effector or target cells only. Propidium iodide was added at 13 μg/tube and the tubes were incubated in a 5% CO_2 atmosphere, at 37°C, for 2 h. Detection of target cells was done by flow cytometry using two-parameter dot plots. Damaged target cells were identified as the doubly labeled (green and red) cells. NK cells remains unstained and intact target cells are stained green only. Percentage of specific lysis was calculated by determining the fraction (%) of dead target cells subtracted from % of debris and fragments. NK activity was expressed as the number of lytic units 40% per 10^7 cells. A single assay was performed on triplicate for the patient and control children ($n = 10$).

CD8+ T Cell Cytotoxicity and Degranulation Assays

In order to obtain IL-2-dependent T cells, patient and control cells were stimulated for 24 h, with 3 μg/mL of PHA (Difco; Surrey, UK) in PANSERIN medium (Biotech GMBH; Berlin, Germany) supplemented with 5% Human AB serum and 40 IU/mL IL-2 (PeproTech; London, UK), under standard cell culture conditions. Then, cells were maintained in culture for an additional 6 day period under the same conditions, except for the absence of PHA. For assaying the cytotoxic activity, we measured the lysis of Fas-deficient L1210-3 target cells in a standard 4 h ^{51}Cr-release assay in the presence of a monoclonal antibody to CD3 (10 μg, OKT3, Ortoclone, Belgium), after incubation with different ratios of effector/target cells, as described by Stepp *et al.* (37). For the degranulation assay, 6×10^3 cells were plated in wells coated with anti-CD3 (OKT3, 20 μg/mL) and incubated for 4 h. The *N*-a-benzyloxycarbonyl-L-lysine thiobenzyl ester (BLT) esterase (granzyme A) activity on a 50-μL aliquot of cell-free supernatant was measured (41). The effector/target ratio was calculated from the number of CD8 + T cells, as determined by flow cytometry using a FACScan equipment (Becton-Dickinson, San Jose, USA). These assays were done once, in quadruplicate, using cells from the patient and a single healthy control of matched age.

Cloning Strategies for Obtaining the Retroviral Vector and Rab27a Construct

We cloned the RAB27A cDNA into the pBS-MFGB2-IRES-EGFP vector, constructed and kindly given to us by Dr. Frédéric Rieux-Laucat, from the INSERM U-429, Paris, France. In order to obtain the vector, the HindIII-EcoRI fragment of the GC-B2 plasmid (containing the Mo-MLV DNA)(42) was subcloned into the HindIII-EcoRI sites of pBluescript SK (pBS-MFG-B2). In addition, a NcoI-BglII IRES-EGFP cassette was subcloned from a PCR-modified pIRES2-EGFP into the NcoI-BamHI sites of pBS-MFG-B2 (pBS-MFGB2-IRES-GFP). RAB27A sequence was amplified using strategic primers containing a 5′ AflIII site and a 3′ BamHI site (5′-GGG GGA CAT GTC TGA TGG AGA TTA TGA-3′ and 5′-GCG GAT CCG CCC ACC TGA ACT ACT ATG TCA-3′) and subcloned into the pGEM-T easy vector system I (Promega, Madison, USA). The insert was digested from pGEM with AflIII and BamHI and ligated into the NcoI (compatible with AflIII) and BamHI sites in the pBS-MFGB2-IRES-GFP vector constructed. The clone was confirmed by sequencing, and preparative amounts of purified plasmids (Rab27a construct and vector alone) were obtained by Maxi-preparation (QIAGEN, Valencia, USA).

Transfection of Packaging Phoenix Cells

Transfection of Phoenix cells (43) was done using FUGENE^{TM} 6 Transfection kit (Roche, Mannheim, Germany), in semiconfluent 10 cm culture dishes (NUNC, Naperville, USA). Three different conditions were assayed: RAB27A construct, vector alone, and no plasmid. After 24 and 48 h, the medium was collected, filtered in a 0.22 μm filter and frozen at –80°C. These retroviral supernatants were used to infect T cells. The percentage of Phoenix transfected cells was estimated by flow cytometry.

Transduction of IL2-Dependent T Cells with Retroviral Particles

Human Fibronectin (Sigma, St. Louis, USA) coated 6-well plates (COSTAR, Cambridge, England) were used to plate 8×10^5 IL2-dependent T cells, cultured for 7 days, as describe above. After 24 h, the medium was replaced by the retroviral supernatants supplemented with 4 mg/mL of protamine sulfate (Sigma, St. Louis, USA). Three cycles of infection, 12 h each, were done by replacing the supernatant, and after 48 h from the last cycle, the cells were submitted to the cytotoxicity assay as described above. The percentage of transduced cells was estimated by flow cytometry using the GFP fluorescence as a reference.

Statistical Analysis

In order to statistically compare immunological parameters (lymphocyte proliferation, NK activity and HLA-DR expression), as well as levels of myosin-Va expression in immune cells, between the patient and controls, we calculated and indicated on the graphs, the percentiles 25 and 75 from the control data set. All calculations were performed using the Prism 2.01 software.

RESULTS

Cellular Diagnosis of Griscelli Syndrome

A photograph of the patient when he was 4-years-old (with authorization from his parents) is shown in Fig. 1A. The silvery-gray hair is noticeable over the head, face, eyelashes, and eyebrowns. Also his skin appears to be hypopigmented as compared with his brother and parents (not shown). Direct examination of the hair under an optical microscope showed abnormal distribution of pigments, characterized by the presence of large clumps of pigments and extended areas free of pigment in the shaft (Fig. 1B), compared with the homogeneous distribution of pigment in the hair shaft from a normal control individual (Fig. 1C). This pigmentation pattern of the hair is observed in all GS patients and can be used as a differential diagnosis between other pigmentary diseases, such as CHS, which is characterized by the presence of small aggregates of pigments distributed throughout the hair shaft (1). Hematoxylin-eosin stained skin sections observed under the optical microscope revealed the presence of highly pigmented, dark melanocytes, in the basal layer of the epidermis (Fig. 1D). In contrast, the melanocytes of normal skin appear as clear cells not distinguished from the surrounding keratinocytes (Fig. 1E). Electron microscopic observation revealed melanosomes of normal size and morphology, but densely accumulated in the cell body of the melanocytes (Fig. 1F), markedly distinct from the large inclusions observed in CHS (1).

The Patient Carries Two Different Mutant Alleles of the RAB27A Gene

Exons 2–6 and flanking regions of *RAB27A* gene of the patient were sequenced and analyzed, leading to the identification of two heterozygous mutations in this gene (Fig. 2A). One allele has a C-T transition on exon 5,

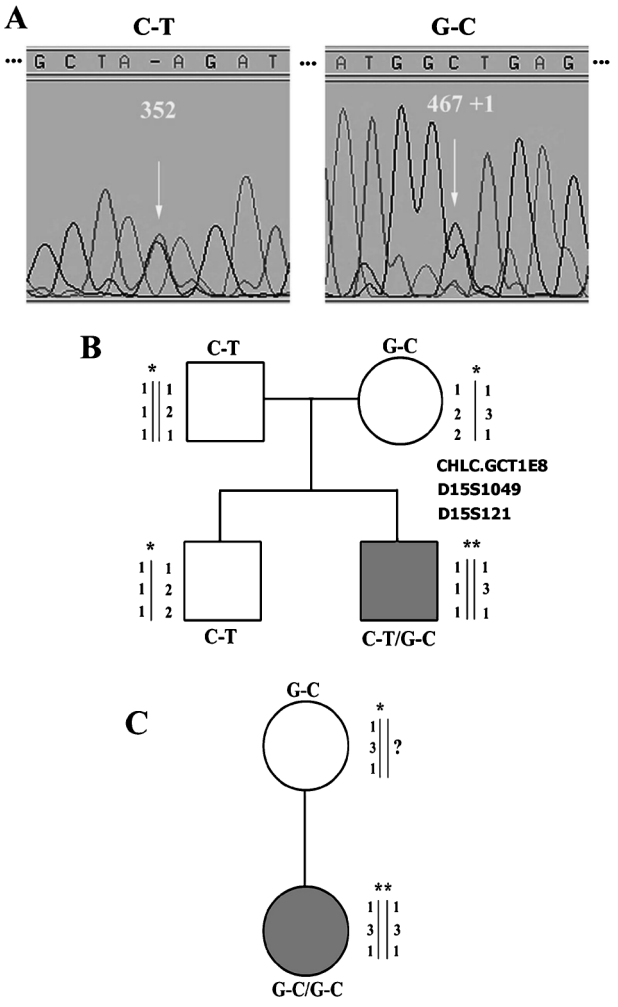

Fig. 2. Mutations detected in the Rab27a gene and pedigree analysis. (A) Electrophoregrams showing the genomic sequence from two regions of the *RAB27A* gene. The two mutations detected (C352T and G467 + 1 C) are indicated by arrows. (B and C) Pedigree from the patient's family (B) and a second Brazilian family (C) and segregation analysis of the polymorphic markers linked to the GS2 locus on chromosome 15q21. Asterisks indicate affected haplotypes. Note that the mothers share common marker haplotype. [Note: The on-line version of this figure appears in color.]

corresponding to position 352 on the RAB27A cDNA. This nonsense mutation leads to a STOP codon, TAG, in place of a CAG codon, which encodes for the Glutamine 118 in the predicted Rab27a amino acid sequence. The predicted amino acid sequence of the human Rab27a protein is 221 amino acids. The other allele contains a G-C transversion on the splicing donor site of exon 5, in the position 467 + 1. This mutation will probably interfere with mRNA splicing leading to a frameshift.

Pedigree Analysis

Sequencing and analysis of the *RAB27A* gene of the patient's parents revealed that the C352T mutation was inherited from the father and the G467 + 1C mutation from the mother (data not shown). The second child of this family, who is healthy, carries only the C352T mutation, being therefore, heterozygous for this disease (data not shown). On the basis of this data, the family was advised regarding the risks of conceiving other children carrying this disease. Polymorphic markers were used to identify a possible relation between this family and another Brazilian family carrying the G467 + 1C mutation, which had previously been determined (4). The pedigree of the family described in the present work, with the mutations and polymorphic markers indicated, is shown in Fig. 2B, and the pedigree for the second family is shown in Fig. 2C. Note that the mothers share common marker haplotypes within a small genetic region of the *RAB27A* locus, suggesting that the mutation arose from a common ancestor.

Patient Lymphocytes are Capable of Responding to Mitogens and Alloantigens

Our results show that the patient's circulating lymphocytes are capable to proliferate when stimulated by mitogens or alloantigens (Fig. 3A and B). Patient cells incorporated ^{3}H-Thymidine under stimuli by PHA (17,500 cpm) and Con-A (24,780 cpm), presenting stimulation index of 28 and 34, respectively. Median values from 10 control individuals were 12,480 cpm for PHA and 12,630 for Con-A stimuli, giving stimulation index of 22 and 18.8, respectively. We also verified that the patient's circulating lymphocytes presented an elevated rate of spontaneous proliferation (2500 cpm) compared to controls, which was on the order of 520 cpm (median from 10 individuals). Therefore, patient lymphocytes showed a proliferation rate and stimulation index above control range for both mitogens (Fig. 3A), whereas, in the mixed lymphocyte cultures (Fig. 3B), similar rates of lymphocyte prolif-

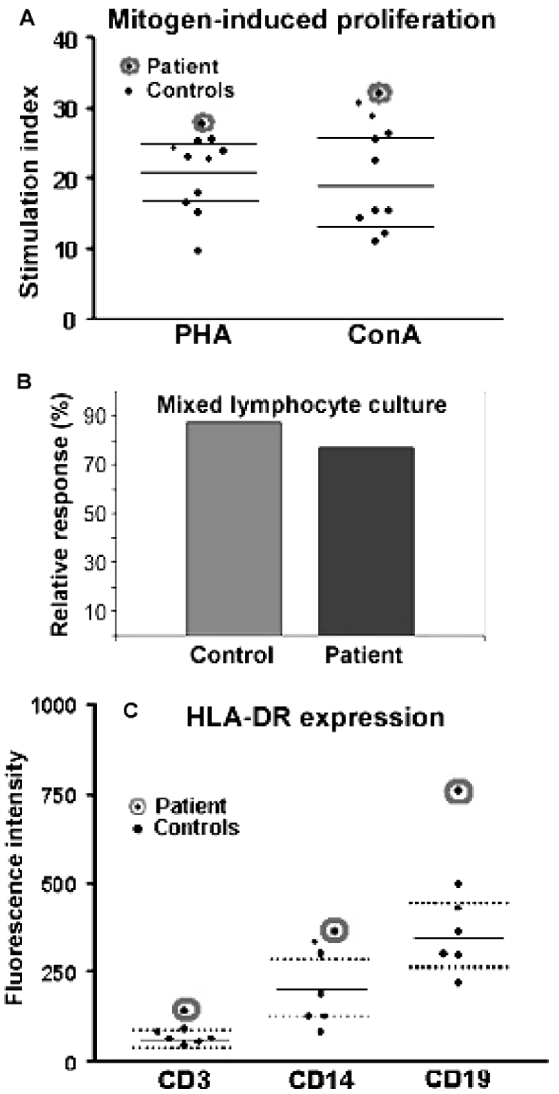

Fig. 3. Lymphocyte proliferation in response to mitogens or alloantigens and surface expression of HLA-DR. (A) Stimulation index for PHA or Con-A induced lymphocyte proliferation in peripheral blood lymphocytes from the patient and 10 controls. Median and the percentiles 25 and 75 from the control data points are indicated by horizontal lines. (B) Proliferation relative response to alloantigens stimulation (mixed lymphocyte cultures). Note that patient lymphocytes showed proliferation indices above control range in response to both mitogens but not to alloantigens. (C) Flow cytometric quantification of HLA-DR staining on CD3, CD14 and CD19 cell subsets in the patient and 6 control children. The mean and standard deviation (SD) values of the median of fluorescence intensity for the patient's CD3 (135, SD = 2.8), CD14 (345.5, SD = 4.2), and CD19 (757, SD = 15.5) cell subsets were obtained from three independent assays. Median values from the 6 control data points (CD3 = 61.3, CD14 = 193.3 and CD19 = 332.4) and the percentiles 25 and 75 are indicated by horizontal lines.

eration were obtained for the patient (relative response = 79%) or control cells (relative response = 86%).

HLA-DR Expression Suggests an Activation Status of the Patient Lymphocytes

Fluorescence intensity for the surface staining of HLA-DR molecules on nonstimulated T or B lymphocytes (CD3 or CD19) or monocytes (CD14) is plotted in Fig. 3C, for the patient and the control children ($n = 6$). This analysis shows that HLA-DR expression on the patient cells is above control range. HLA-DR expression on CD3 cells suggests an activation status of these circulating lymphocytes.

Differential Myosin-Va Expression and Localization: A Functional Link with Rab27a in Lymphocytes or a Result of Lymphocyte Activation?

To test the originally proposed working hypothesis of *MYO5A* gene mutation we analyzed myosin-Va protein expression in the mononuclear blood cells of the patient. The polypeptide of expected size was detected in Western blots (data not shown). Also, flow cytometry showed staining for myosin-Va in all mononuclear cell subsets (Fig. 4A). The results (in Fig. 4A) suggest an increase in myosin-Va levels in the patient cells, most prominent in lymphocytes and monocytes, in comparison with adult control individuals. Given the association of myosin-Va and Rab27a in melanocytes and the high levels for myosin-Va shown here we reasoned that it would be important to characterize the cellular localization of myosin-Va in the patient's mononuclear cells. Confocal microscopy images of myosin-Va staining (Fig. 4B–E) shows a typical punctate distribution of myosin-Va throughout the cytoplasm and also remarkably colocalized with the microtubule organizing center in both mutant or control lymphocytes. In several instances centrosomal staining for myosin-Va appeared to be more striking in the patient lymphocytes than in controls (see Fig. 4 B–D).

Cytotoxic Response Is Impaired in the Patient's NK and CD8+ Cells

NK and T cell cytotoxic activities are dependent on lytic granule release. The NK cytotoxic activity against K562 target cells (Fig. 5A), assessed by flow cytometry, was shown to be about 1.5-fold lower in the patient cells compared with the control median from 10 control children, while this is not a remarkable deficiency it is below the activity found in every control individual. By the ^{51}Cr-release assay, we found that the cytotoxic activity of IL2-dependent, CD8+ T cells against Fas-deficient L1210-3 target cells (Fig. 5B) was on the order of 3- to 5-fold lower in the patient cells compared with the control. Also, the degranulation activity of the CD8+ T cells (Fig. 5C) from the patient was markedly lower than the control.

Retroviral Gene Transfer Restores Cytotoxicity of RAB27A Mutant T Cells

RAB27A cDNA was cloned into the retroviral vector pBSMFGB2IresEGFP and Phoenix packaging cells were transfected as shown in Fig. 6A. Around 50% of the cells were transfected and the supernatant was collected 24 and 48 h after transfection and used to infect the patient's IL2-dependent T cells. After three cycles of infection, the proportion of transduced cells was about 10%, as analyzed by flow cytometry (Fig. 6B). The cytotoxic activity of these cells was then measured, and as shown in Fig. 6C, rescue of the cytoxic function of patient cells was obtained upon RAB27A transduction, which was not observed upon GFP transduction.

DISCUSSION

Griscelli syndrome is a rare and not widely known disease. Its diagnosis has been often incorrectly made due to the remarkable similarity of symptoms with Chediak-Higashi syndrome or Familial Hemophagocytic lymphohistiocytosis. Examination of the pigment alterations within the hair shaft and skin melanocytes led us to establish the differential diagnosis between these diseases (Fig. 1), as previously indicated by several authors (1, 2, 8). On the basis of a previous report on the involvement of *MYO5A* gene with GS (7), we first searched for mutations in this gene, which was, however, found to be intact (data not shown). More recent studies (4, 14) then led us to direct our search for mutations towards *RAB27A*. Evaluation of the clinical history of the patient described here was clearly indicative of GS2 subtype, i.e., caused by *RAB27A* mutation. We found two heterozygous mutant alleles of *RAB27A* in this patient, a C352T mutation inherited from the father and a G467 + 1C mutation, from the mother (Fig. 2). Ménasché *et al.* (4) have previously characterized a homozygous G467 + 1C mutation in a Brazilian child. Since both patients' mother are heterozygous for this mutation and share the same marker haplotypes, this finding is compatible with a mutation inherited from a common ancestor. The patient's brother without disease expression was heterozygous for paternal *RAB27A* mutation and affected haplotype. These findings were used in genetic counseling to the family. Interestingly, a nonsense mutation C346T (Q116stop), close to the

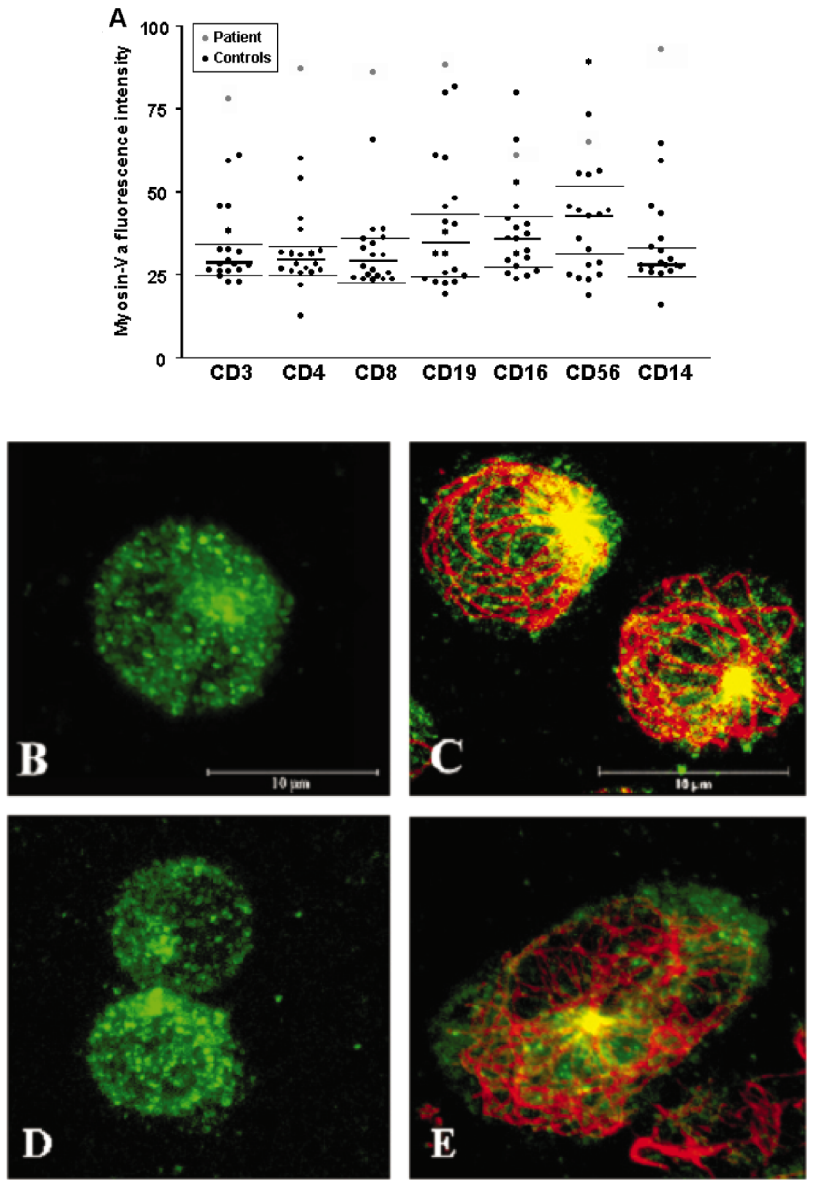

Fig. 4. Expression and localization analyses of myosin-Va in mononuclear cells. (A) Median of myosin-Va fluorescence intensity, measured by flow cytometry, in mononuclear cells from the patient, compared to 19 healthy, adult blood donors (controls). Median values from the control data points for all cell subsets and the percentiles 25 and 75 are indicated by horizontal lines. (B–E) Confocal microscopy images of myosin-Va staining (green) alone (B and D) or superimposed images of the myosin-Va (green) and β-tubulin (red) staining (C and E). The images were generated from reconstruction of multiple optical sections. Note that myosin-Va has a typical punctate distribution throughout the cytoplasm in both patient and control lymphocytes, but its accumulation in the centrosome appears to be more intense in the patient cells.

C352T (Q118stop) identified here, was previously identified leading to lymphohistiocytic infiltration, low platelet levels, and secondary neurological symptoms with onset at 1-year-old (6). Regarding the effects of these mutations in mRNA and protein expression, no characterization has been done either for the patient describe here or for the previous patients (4, 6). In order to characterize these mutant alleles and be able to make functional or clinical correlations it will be necessary to determine whether the mRNA and a truncated Rab27a protein are detected.

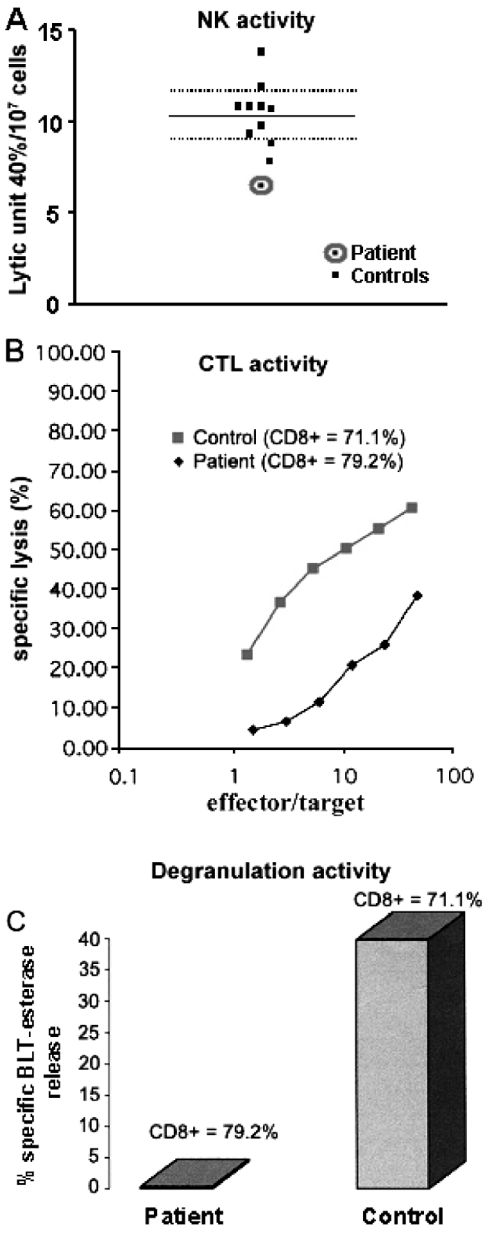

Fig. 5. Defective cytotoxic activity in NK and CTLs from the patient with *RAB27A* mutation. (A) NK cytotoxic activity against K562 target cells, assessed by flow cytometry. The values of the lytic unit 40% per 10^7 cells obtained from a single assay for the patient (6.5) and 10 control healthy chidren are plotted, and the median (10.33) from the control data points as well as the percentiles 25 and 75 (8.6 and 11.5) are indicated by horizontal lines. (B) Cytotoxic activity of CD8+ T lymphocytes against Fas-deficient L1210-3 target cells. (C) Degranulation activity of CD8+ T lymphocytes. The relative number of CD8+ cells in the patient (79.2%) and control (71.1%) samples is indicated. BLT esterase activity was measured in the cell supernatants. The % of specific BLT esterase release was calculated according to the formula: (specific activity in the supernatant of the anti-CD3 activated cells – spontaneous release)/(activity in the total cell lysate – spontaneous release) × 100, where spontaneous release was obtained from nonactivated cells.

The observation of an elevated rate of spontaneous and mitogen-induced proliferation and the high expression of HLA-DR molecules on lymphocyte and monocyte cell surfaces (Fig. 3) are compatible with generalized lymphocyte and macrophage activation leading to HS in this patient. It is generally accepted that the "spontaneous" lymphocyte proliferation (potentially triggered by an infectious agent), causing HS in GS2 patients, is a consequence of the lack of T cell cytotoxic activity, although the precise mechanism is not fully understood (44). Our results are also consistent with a strong deficiency in CD8+ T cell cytotoxicity associated with *RAB27A* mutation, as previously shown (4, 35, 36). Additionally, we show a deficiency in NK cytotoxic activity in this patient (Fig. 5), compatible with the interpretation that both CD8+ and NK cells citotoxicity rely on Rab27a-dependent mechanisms for lytic granule release. We have not an explanation to why the NK deficiency shown here was subtle compared to the deficiency found in CD8+ cells. One possibility is that the flow cytometric analysis used for NK activity also detects cell damage induced by a lytic granule independent pathway, though we can not rule out the possibility of an alternative overlapping mechanism playing a function in NK cells.

Although myosin-Va is not required for the cytotoxic activity (4, 35, 36), we found it pertinent to report here our findings, since they suggest an increase in the myosin-Va levels and a more prominent centrosomal staining for this myosin in the *RAB27A* mutant lymphocytes (Fig. 4). Despite that the flow cytometric analysis was not done with a matched age control group, nor could it be repeated due to limitation in obtaining cells from the patient, this finding is consistent with previously reported evidence of higher myosin-Va levels in *RAB27A* mutant fibroblasts (13). The patient lymphocytes exhibited a typical punctate distribution pattern of myosin-Va, though a more prominent centrosomal staining was often noted. In spite that future studies will be necessary to confirm this observation, an accumulation of myosin-Va at the centrosomal region is consistent with previously reported results on *RAB27A* mutant melanocytes (45). These findings might simply be related to lymphocyte activation, since an increase in myosin-Va expression in response to lymphocyte activation has been demonstrated (33). Lymphocyte activation is one of the main concerns in this pathological condition, and is in fact likely to occur in this patient as discussed above. On the other hand, these results could be interpreted as due to a feedback mechanism that compensates for the lack of function of Rab27a GTPase or a decreased turnover of the myosin-Va protein. Since *MYO5A* mutations do not affect the degranulation pathway of cytotoxic cells, either

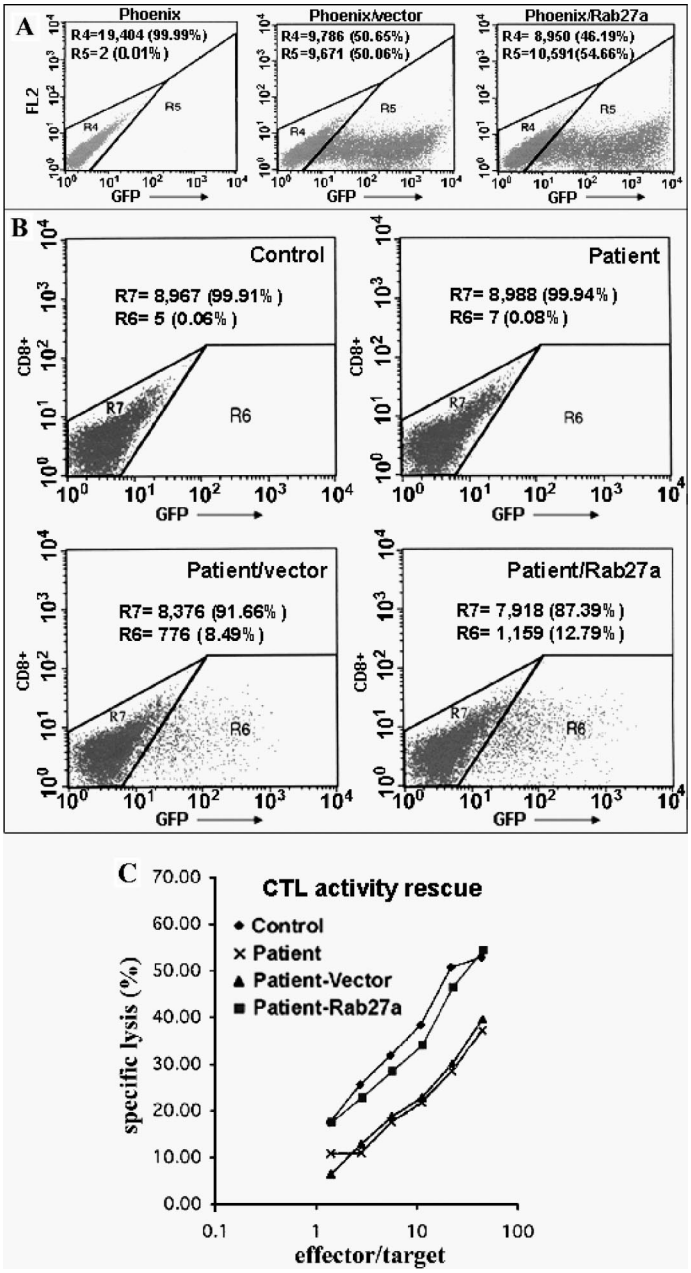

Fig. 6. Restoration of the cytotoxic activity upon transduction of the patient's CD8+ lymphocytes with retrovirus carrying the RAB27A cDNA. (A) Quantification of transfected Phoenix cells by GFP detection, using flow cytometry. R4 indicates the nontransfected cell population (GFP negative). R5 indicates the population of cells expressing GFP (GFP positive). (B) Quantification of T cells infected with the retrovirus particles produced by the PHOENIX cells. R7 indicates the GFP negative population of cells and R6 represents the GFP positive cells. (C) Cytotoxic activity of IL2-dependent T cells against Fas-deficient L1210-3 target cells. Note that the cytotoxic activity of the Rab27a-retrovirus infected cells is comparable to healthy control cells, whereas the patient's cells infected with GFP-retrovirus or noninfected cells showed low levels of activity. The percentage of CD8+ cells, as measured by FACS, was: Control = 73.3%; Patient = 74.5%; Patient-Vector = 75.20%; Patient-Rab27a = 76.6%. Cells were cultured for 10 days.

myosin-Va plays a complementary role in this function or its connection with Rab27a suggested here involves additional lymphocyte Rab27a-dependent function(s). Although these possibilities are intriguing, elucidation of myosin-Va function in lymphocytes is beyond the scope of this work.

One of the most important aspects of the present work was to demonstrate the rescuing of T lymphocyte cytotoxic activity, using retroviral vector mediated gene transfer, which was successful in restoring *in vitro* the cytotoxic function of *RAB27A* mutant CD8+ T cells, even with only about 10% of the cells being expressing the retroviral GFP-IRES-Rab27a. This is not surprising, since the efficacy of T lymphocyte cytotoxic activity is remarkable, and cytotoxic cells have the ability to kill several target cells in few minutes. Thus even a few cytotoxic cells may be highly efficient. Hence, this functional rescue confirms that the mutations mapped in the *RAB27A* gene are those responsible for the lack of cytotoxic activity in CD8+ T lymphocytes of this patient and also strengthens that Rab27a GTPase plays indeed an essential role in the lytic granule release. The correction shown was done with transiently transduced T cells not allowing detection of the protein level or further functional studies. Although the expression of GFP is not an absolute proof of Rab27a expression, a unique RNA containing both genes (GFP and Rab27a) is produced and then processed in IRES system. Additionally, since a correction of the cytotoxicity is observed in GFP-IRES-RAB27a and not with GFP-IRES alone, it is difficult to conceive that Rab27a was not properly expressed. Therefore, the data shown here represent the first step in evaluation of the feasibility of acute phase treatment of GS2 patients, using genetically modified cytotoxic T lymphocytes. Until now the first choice of treatment for GS2 has been bone marrow transplantation when possible (17, 18). Alternatively, chemotherapy has been used in order to maintain the patient in long-term remission (19, 20). Undoubtedly, efforts towards finding an efficient treatment, available and applicable for all patients are desirable. In future experiments aiming at genetic correction of these cells, stable transfection of the cells will be required. The ashen mice, the natural Rab27a murine mutant, may be a useful model to evaluate *in vivo* the possibilities of *RAB27A* gene correction approaches.

ACKNOWLEDGMENTS

We especially thank: Dr. Frédéric Rieux-Laucat, who kindly gave us the retroviral vector used in this work. Silmara Reis Banzi for excellent technical assistance. Maria D. Seabra Ferreira, Maria Tereza P. Maglia, José Augusto Maulin, Izilda R. Violante, Vani M. Alves Correia, and Márcia Graeff from the optical and electron microscopy laboratories of the Departamento de Biologia Celular e Molecular e Bioagentes Patogênicos-FMRP-USP; Patricia Vianna Bonini Palma and Fabiana Rosseto de Morais, from FUNDHERP, for the flow-cytometry expertise; Nathalie Lambert and Stéphanie Certain, from Hôspital Necker Enfants Malades and INSERM-U429. Grant Support: This work was supported by FAPESP, CNPq, FUNDHERP, FAEPA, and UNAERP, in Brazil, and INSERM in France.

REFERENCES

1. Griscelli C, Durandy A, Guy-Grand D, Daguillard F, Herzog C, Prunieras M: A syndrome associating partial albinism and immunodeficiency. Am J Med 65:691–702, 1978
2. Klein C, Philippe N, Le Deist F, Fraitag S, Prost C, Durandy A, Fischer A, Griscelli C: Partial albinism with immunodeficiency (Griscelli syndrome). J Pediatr 125:886–895, 1994
3. Bahadoran P, Aberdam E, Mantoux F, Busca R, Bille K, Yalman N, Saint-Basile G, Casaroli-Marano R, Ortonne JP, Ballotti R: Rab27a: A key to melanosome transport in human melanocytes. J Cell Biol 152:843–850, 2001
4. Ménasché G, Pastural E, Feldmann J, Certain S, Ersoy F, Dupuis S, Wulffraat N, Bianchi D, Fischer A, Le Deist F, de Saint-Basile G: Mutations in RAB27A cause Griscelli syndrome associated with haemophagocytic syndrome. Nat Genet 25:173–176, 2000
5. de Saint Basile G: Implication du traffic intracellulaire dans troiss maladies héréditaires du syst'eme hématopoïétique. Méd Sci 16:745–750, 2000
6. Sanal O, Ersoy F, Tezcan I, Metin A, Yel L, Menasche G, Gurgey A, Berkel I, de Saint-Basile G: Griscelli disease: Genotype–phenotype correlation in an array of clinical heterogeneity. J Clin Immunol 22:237–243, 2002
7. Haraldsson A, Weemaes CM, Bakkeren JA, Happle R: Griscelli disease with cerebral involvement. Eur J Pediatr 150:419–422, 1991
8. Pastural E, Barrat FJ, Dufourcq-Lagelouse R, Certain S, Sanal O, Jabado N, Seger R, Griscelli C, Fischer A, de Saint-Basile G: Griscelli disease maps to chromosome 15q21 and is associated with mutations in the myosin-Va gene. Nat Genet 16:289–292, 1997
9. Mercer JA, Seperack PK, Strobel MC, Copeland NG, Jenkins NA: Novel myosin heavy chain encoded by murine dilute coat colour locus. Nature 349:709–713, 1991
10. Titus MA: Motor proteins: Myosin-V the multi-purpose transport motor. Curr Biol 7:R301–R304, 1997
11. Reck-Peterson SL, Tyska MJ, Novick PJ, Mooseker MS: The yeast class V myosins, Myo2p and Myo4p, are nonprocessive actin-based motors. J Cell Biol 153:1121–1126, 2001
12. Langford GM: Myosin-V, a versatile motor for short-range vesicle transport. Traffic 3:859–865, 2002
13. Pastural E, Ersoy F, Yalman N, Wulffraat N, Grillo E, Ozkinay F, Tezcan I, Gedikoglu G, Philippe N, Fischer A, de Saint-Basile G: Two genes are responsible for Griscelli syndrome at the same 15q21 locus. Genomics 63:299–306, 2000
14. Wilson SM, Yip R, Swing DA, O'Sullivan TN, Zhang Y, Novak EK, Swank RT, Russell LB, Copeland NG, Jenkins NA: A mutation in

Rab27a causes the vesicle transport defects observed in ashen mice. Proc Natl Acad Sci USA 97:7933–7938, 2000
15. Deacon SW, Gelfand VI: Of yeast, mice, and men. Rab proteins and organelle transport. J Cell Biol 152:F21–F24, 2001
16. Seabra MC, Mules EH, Hume AN: Rab GTPases, intracellular traffic and disease. Trends Mol Med 8:23–30, 2002
17. Schneider LC, Berman RS, Shea CR, Perez-Atayde AR, Weinstein H, Geha RS: Bone marrow transplantation (BMT) for the syndrome of pigmentary dilution and lymphohistiocytosis (Griscelli's syndrome). J Clin Immunol 10:146–153, 1990
18. Tezcan I, Sanal O, Ersoy F, Uckan D, Kilic S, Metin A, Cetin M, Akin R, Oner C, Tuncer A: Successful bone marrow transplantation in a case of Griscelli disease which presented in accelerated phase with neurological involvement. Bone Marrow Transplant 24:931–933, 1999
19. Gurgey A, Sayli T, Gunay M, Ersoy F, Kucukali T, Kale G, Caglar M: High-dose methylprednisolone and VP-16 in treatment of Griscelli syndrome with central nervous system involvement. Am J Hematol 47:331–332, 1994
20. Imashuku S, Hibi S, Ohara T, Iwai A, Sako M, Kato M, Arakawa H, Sotomatsu M, Kataoka S, Asami K, Hasegawa D, Kosaka Y, Sano K, Igarashi N, Maruhashi K, Ichimi R, Kawasaki H, Maeda N, Tanizawa A, Arai K, Abe T, Hisakawa H, Miyashita H, Henter JI: Effective control of Epstein-Barr virus-related hemophagocytic lymphohistiocytosis with immunochemotherapy. Blood 93:1869–1874, 1999
21. Anikster Y, Huizing M, Anderson PD, Fitzpatrick DL, Klar A, Gross-Kieselstein E, Berkun Y, Shazberg G, Gahl WA, Hurvitz H: Evidence that Griscelli syndrome with neurological involvement is caused by mutations in RAB27A, not MYO5A. Am J Hum Genet 71:407–414, 2002
22. Matesic LE, Yip R, Reuss AE, Swing DA, O'Sullivan TN, Fletcher CF, Copeland NG, Jenkins NA: Mutations in Mlph, encoding a member of the Rab effector family, cause the melanosome transport defects observed in leaden mice. Proc Natl Acad Sci USA 98:10238–10243, 2001
23. Ménasché G, Ho CH, Sanal O, Feldmann J, Tezcan I, Ersoy F, Houdusee A, Fisher A, de Saint-Basile G: Griscelli syndrome restricted to hypopigmentation results from a melanophilin defect (GS3) or a MYO5A F-exon deletion (GS1). J Clin Invest 112:450–456, 2003
24. Wu XS, Rao K, Zhang H, Wang F, Sellers JR, Matesic LE, Copeland NG, Jenkins NA, Hammer JA, III: Identification of an organelle receptor for myosin-Va. Nat Cell Biol 4:271–278, 2002
25. Nagashima K, Torii S, Yi Z, Igarashi M, Okamoto K, Takeuchi T, Izumi T: Melanophilin directly links Rab27a and myosin Va through its distinct coiled-coil regions. FEBS Lett 517:233–238, 2002
26. Fukuda M, Kuroda TS, Mikoshiba K: Slac2-a/melanophilin, the missing link between Rab27 and myosin Va: Implications of a tripartite protein complex for melanosome transport. J Biol Chem 277:12432–12436, 2002
27. Provance DW, Jr, James TL, Mercer JA: Melanophilin, the product of the Leaden locus, is required for targeting of myosin-Va to melanosomes. Traffic 3:124–132, 2002
28. Nascimento AA, Roland JT, Gelfand VI: Pigment cells: A model for the study of organelle transport. Annu Rev Cell Dev Biol 19:469–491, 2003
29. Hume AN, Collinson LM, Hopkins CR, Strom M, Barral DC, Bossi G, Griffiths GM, Seabra MC: The leaden gene product is required with Rab27a to recruit myosin Va to melanosomes in melanocytes. Traffic 3:193–202, 2002
30. Espindola FS, Espreafico EM, Coelho MV, Martins AR, Costa FR, Mooseker MS, Larson RE: Biochemical and immunological characterization of p190-calmodulin complex from vertebrate brain: A novel calmodulin-binding myosin. J Cell Biol 118:359–368, 1992
31. Reis D, Souza M, Mineo J, Espindola F: Myosin V and iNOS expression is enhanced in J774 murine macrophages treated with IFN-gamma. Braz J Med Biol Res 34:221–226, 2001
32. Rodriguez OC, Cheney RE: Human myosin-Vc is a novel class V myosin expressed in epithelial cells. J Cell Sci 115:991–1004, 2002
33. Bizario JC, Castro FA, Sousa JF, Fernandes RN, Damiao AD, Oliveira MK, Palma PV, Larson RE, Voltarelli JC, Espreafico EM: Myosin-V colocalizes with MHC class II in blood mononuclear cells and is up-regulated by T-lymphocyte activation. J Leukoc Biol 71:195–204, 2002
34. Strom M, Hume AN, Tarafder AK, Barkagianni E, Seabra MC: A family of Rab27-binding proteins. Melanophilin links Rab27a and myosin Va function in melanosome transport. J Biol Chem 277:25423–25430, 2002
35. Haddad EK, Wu X, Hammer JA, III, Henkart PA: Defective granule exocytosis in Rab27a-deficient lymphocytes from Ashen mice. J Cell Biol 152:835–842, 2001
36. Stinchcombe JC, Barral DC, Mules EH, Booth S, Hume AN, Machesky LM, Seabra MC, Griffiths GM: Rab27a is required for regulated secretion in cytotoxic T lymphocytes. J Cell Biol 152:825–834, 2001
37. Stepp SE, Dufourcq-Lagelouse R, Le Deist F, Bhawan S, Certain S, Mathew PA, Henter JI, Bennett M, Fischer A, de Saint-Basile G, Kumar V: Perforin gene defects in familial hemophagocytic lymphohistiocytosis. Science 286:1957–1959, 1999
38. Bach FH, Bach ML: Mixed lymphocyte cultures in transplantation immunology. Transplant Proc 3:942–948, 1971
39. Espreafico EM, Cheney RE, Matteoli M, Nascimento AAC, de Camili PV, Larson RE, Mooseker MS: Primary structure and cellular localization of chicken brain myosin-V (p190), an unconventional myosin with calmodulin light chains. J Cell Biol 119:1541–1558, 1992
40. Chang L, Gusewitch GA, Chritton DB, Folz JC, Lebeck LK, Nehlsen-Cannarella SL: Rapid flow cytometric assay for the assessment of natural killer cell activity. J Immunol Methods 166:45–54, 1993
41. Kim S, Yokoyama WM: NK cell granule exocytosis and cytokine production inhibited by Ly-49A engagement. Cell Immunol 183:106–112, 1998
42. Hacein-Bey H, Cavazzana-Calvo M, Le Deist F, Dautry-Varsat A, Hivroz C, Riviere I, Danos O, Heard JM, Sugamura K, Fisher A, de Saint-Basile G: Gamma-c gene transfer into SCID X1 patients' B-cell lines restores normal high-affinity interleukin-2 receptor expression and function. Blood 87:3108–3116, 1996
43. Yang S, Delgado R, King SR, Woffendin C, Barker CS, Yang ZY, Xu L, Nolan GP, Nabel GJ: Generation of retroviral vector for clinical studies using transient transfection. Hum Gene Ther 10:123–132, 1999
44. de Saint-Basile G, Fisher A: The role of cytotoxicity in lymphocyte homeostasis. Curr Opin Immunol 13:549–354, 2001
45. Hume AN, Collinson LM, Rapak A, Gomes AQ, Hopkins CR, Seabra MC: Rab27a regulates the peripheral distribution of melanosomes in melanocytes. J Cell Biol 152:795–808, 2001